Nie, S., Marzilli, L., & Yu, N.-T. (1989) *J. Am. Chem. Soc. 111*, 9256–9258.
Nie, S., Marzilli, P., Marzilli, L., & Yu, N.-T. (1990a) *J. Chem. Soc., Chem. Commun.*, 770–771.
Nie, S., Marzilli, P., Marzilli, L., & Yu, N.-T. (1990b) *J. Am. Chem. Soc. 112*, 6084–6091.
Nexo, E., & Olesen, H. (1976) *Biochim. Biophys. Acta 446*, 143–150.
Nexo, E., & Olesen, H. (1982) in B_{12} *II* (Dolphin, D., Ed.) pp 57–86, J. Wiley & Sons, New York.
Pagano, T., & Marzilli, L. (1989) *Biochemistry 28*, 7213–7223.
Parker, F. (1983) *Applications of Infrared Spectroscopy in Biochemistry*, Plenum Press, London.
Pett, V., Liebman, M., Murray-Rust, P., Prasad, K., & Glusker, J. (1987) *J. Am. Chem. Soc. 109*, 3207–3215.
Pratt, J. (1972) *Inorganic Chemistry of Vitamin* B_{12}, Academic Press, London.
Rajoria, D., & Nath, A (1977) *Inorg. Nucl. Chem. 39*, 1291–1294.
Rossi, M., Glusker, J., Randaccio, L., Summers, M., Toscano, P., & Marzilli, L. (1985) *J. Am. Chem. Soc. 107*, 1729–1738.
Sagi, I., Wirt, M., Chen, E., Frisbie, S., & Chance, M. (1990) *J. Am. Chem. Soc. 112*, 8639–8644.
Salama, S., & Spiro, T. (1977) *J. Raman Spectrosc. 6*, 57–60.
Savage, H., Lindley, P., Finney, J., & Timmins, P. (1987) *Acta Crystallogr. B43*, 296–301.
Toraya, T., Krodel, E., Mildvan, A., & Abeles, R. (1979) *J. Am. Chem. Soc. 101*, 417–426.

Spectroscopic Studies of Myoglobin at Low pH: Heme Structure and Ligation†

J. Timothy Sage, Dimitrios Morikis,‡ and Paul M. Champion*
Department of Physics, Northeastern University, Boston, Massachusetts 02115
Received May 14, 1990; Revised Manuscript Received October 11, 1990

ABSTRACT: We explore heme structure and ligation subsequent to a low-pH conformational transition in sperm whale myoglobin. Below pH 4.0, the iron–histidine bond breaks in metMb and deoxyMb. In MbCO, the majority of the iron–histidine bonds remain intact down to pH 2.6; however, the observation of a weak Fe–CO mode at 526 cm^{-1} indicates that a small fraction of the sample has the histidine replaced by a weak ligand, possibly water. The existence of a sterically hindered CO subpopulation in MbCO and the continued association of the four-coordinate heme with the protein in deoxyMb suggest that the heme pocket remains at least partially intact in the acid-induced conformation. The global pH-dependent conformational change described here is clearly distinguished from the local "closed" to "open" transition described previously in MbCO [Morikis et al. (1989) *Biochemistry 28*, 4791–4800]. Further observations of the four-coordinate heme state yield insights on the mechanism of heme photoreduction and the assignment of the 760-nm band in deoxyMb.

Studies of ligand binding to heme proteins are complicated by a variety of factors. For example, we have recently put forward a simple model for ligand binding in heme proteins that formally separates the proximal and distal interactions contributing to the energy barrier for binding at the heme site (Šrajer et al., 1988). The proximal interactions appear to be well explained by use of a simple harmonic approximation to the coordinate describing the iron–porphyrin out-of-plane displacement. Within this model, the distributed low-temperature geminate recombination kinetics of myoglobin (Mb)[1] (Austin et al., 1975), as well as the average heme binding activation energy at physiological temperature, are derived by using heme parameters determined from independent experimental and theoretical studies.

The forces describing the interaction of the ligand with the distal pocket are much more poorly understood. Recent investigations of Mb and hemoglobin (Hb) that utilize the power of site-directed mutagenesis (Morikis et al., 1989; Braunstein et al., 1988; Olson et al., 1989; Nagai et al., 1987) demonstrate, as expected, that the distal histidine plays a significant role in the ligand binding reaction. In fact, it appears that, even at intermediate values of pH (4–7), the distal histidine is coupled to an important protein conformational equilibrium that favors a more "open" and accessible distal pocket structure as the pH is lowered (Morikis et al., 1989). The existence of the open structure has been suggested on the basis of NMR (Lecomte & La Mar, 1985) and X-ray diffraction (Ringe et al., 1984) studies, as well as energetics calculations based on the X-ray structure (Kuriyan et al., 1986).

In the course of our studies, we have become aware of numerous investigations at low pH (2–4) that involve ligand binding to heme model systems (Geibel et al., 1975; Cannon et al., 1976), myoglobin (Giacometti et al., 1977, 1981; Coletta et al., 1985; Traylor et al., 1983; Rousseau et al., 1989; Han et al., 1990) and hemoglobin (Coletta et al., 1988). These investigations are potentially affected by both the proximal and distal interactions discussed above. Proximal interactions may be affected by the alteration of the iron–porphyrin equilibrium displacement that results from loss of the iron–histidine bond (Traylor et al., 1983). Direct resonance Raman evidence that such four-coordinate heme states are formed in

† This work was supported by grants from NSF (87-16382) and NIH (AM-35090).
‡ Present address: Department of Molecular Biology, Research Institute of Scripps Clinic, La Jolla, CA 92037.

[1] Abbreviations: Mb, sperm whale myoglobin; Hb, hemoglobin; metMb, metmyoglobin; deoxyMb, deoxymyoglobin; MbCO, carboxymyoglobin; RR, resonance Raman; CD, circular dichroism; N, native conformation; U, acid conformation, ANS, 1-anilino-8-naphthalenesulfonate.

0006-2960/91/0430-1227$02.50/0

deoxyMb at low pH is presented below. The distal interactions may also be altered at low pH due to global changes in protein conformation (Breslow & Gurd, 1963; Acampora & Hermans, 1967; Puett, 1973; Irace et al., 1986). We show below that such conformations are thermodynamically distinct from the open conformation observed spectroscopically at pH > 4.5 (Ansari et al., 1987; Morikis et al., 1989; Morikis, 1990), even though they may share certain properties (e.g., reduced distal pocket steric hindrance).

The work presented here and in the following paper (Sage et al., 1991) is an attempt to understand in more detail the various interactions and equilibria that must be considered in the low pH regime. We use resonance Raman (RR) spectroscopy to characterize the heme site in low-pH forms of sperm whale metMb, deoxyMb, and MbCO, as well as in the transient photoproduct of MbCO. In addition, circular dichroism (CD) and optical absorption spectra are used to further determine the state of the samples. The characterization of the partially unfolded conformation observed below pH 4 allows us to distinguish it unambiguously from the open conformation studied previously (Morikis et al., 1989). We find that the bond to the proximal histidine is broken in deoxyMb below pH 4. In MbCO, on the other hand, histidine remains ligated in the majority of the proteins. The following paper is devoted to investigation of kinetic and dynamic properties of the low pH myoglobin system.

Experimental Procedures

All samples were prepared from lyophilized sperm whale myoglobin purchased from either Sigma or U.S. Biochemical Corp. MetMb samples were prepared either by dissolving the lyophilized protein directly in the appropriate buffer or by preparing a concentrated unbuffered solution and diluting this solution to the desired concentration in buffer. To produce deoxyMb, metMb samples were thoroughly deoxygenated by flowing Ar or N_2 over the solution, and reduction was accomplished by the addition of sodium dithionite (5–10 μL of a concentrated dithionite solution to approximately 1 mL of 100 μM Mb). MbCO was typically prepared as a 1–2 mM unbuffered solution by dithionite reduction under 1 atm of CO. A small portion of the concentrated MbCO solution was then transferred in a syringe to a sample cell containing CO-saturated buffer. Some MbCO samples were also prepared by flowing CO over the protein solution after reduction; samples prepared by the two procedures were spectroscopically indistinguishable. In the preparation of reduced samples (deoxyMb and MbCO) below pH 4.5, great care must be taken to exclude oxygen from the sample cell due to rapid dithionite degradation and efficient protein oxidation. Sample cells were sealed with rubber septa and paraffin film, and gasses or solutions were introduced through the septa via syringe needles. An additional 5 μL of concentrated dithionite was typically added as a final step in the preparation of all reduced samples in order to eliminate trace amounts of oxygen introduced by the syringe punctures. A Beckman pHI40 pH meter was used to measure the pH of all samples following spectroscopic measurements.

MetMb and deoxyMb samples for Raman measurements were prepared in standard UV quartz fluorometer cells (NSG Precision Cells). For Raman measurements of unphotolyzed MbCO, the sample was prepared in a cylindrical cell and mounted on a spinning shaft in order to minimize CO photolysis. Continuous wave excitation was provided by pumping a dye laser (Coherent CR-599) containing Stilbene 3 with the UV lines of an argon laser (Coherent Innova-100). In all Raman measurements, light scattered at 90° from the incident beam was collected and focused onto the entrance slit of a triple monochromator (Spex Industries). After dispersion in the monochromator, the spectrum of the scattered light was recorded by using an optical multichannel analyzer (Princeton Instruments) interfaced to a personal computer. Frequency calibrations were performed by using Raman lines from fenchone and all reported frequencies are accurate to ± 1 cm^{-1}. Absorption measurements were recorded by using a double-beam spectrophotometer (Perkin-Elmer 320), and CD measurements were performed on a Jasco J-500 spectropolarimeter.

Results

MetMb and DeoxyMb. At pH $\leq$ 4, the optical absorption spectra of both metMb and deoxyMb undergo dramatic changes (Figure 1a,b). Most noticeably, the Soret bands broaden substantially and the absorption maxima shift from 409 to 370 nm (in metMb) and from 434 to 383 nm (in deoxyMb). Other spectral changes are also apparent. In particular, the conformation-sensitive near-IR band that appears at 761 nm in deoxyMb at neutral pH shifts to 775 nm at pH $\leq$ 4 (inset to Figure 1e). Throughout the range pH 2.5–7.5, the observed steady-state absorption spectra for both metMb and deoxyMb can be described as a superposition of the spectra shown in Figure 1a,b, in agreement with previous work that successfully described the pH-dependent thermodynamic and spectroscopic properties of metMb as an equilibrium between two stable conformational states (Acampora & Hermans, 1967; Puett, 1973). We have analyzed the absorption spectra recorded as a function of pH in terms of such a two-state equilibrium between the N (native) state seen at neutral pH and the U (partially unfolded) state observed at low pH, and we display the results in Figure 1d,e.

The cooperative structural transition observed in metMb at low pH is primarily driven by the protonation of histidine residues that are inaccessible to solvent in the native conformation (Breslow & Gurd, 1962). For the purposes of the present work, we describe the N $\rightleftarrows$ U equilibrium by using a simple extension of the coupled protonation/conformation model used previously to describe the equilibrium between the open and closed substates of the N conformation (Morikis et al., 1989). This model is described in detail in the Appendix. The results shown in Figure 1d,e are fit with eq A.3, by using the values $n = 6$, $pK_N = 3.0$, and $pK_U = 5.9$ derived by Puett (1973) in a careful spectroscopic titration of metMb and by allowing pK_{eff} to vary in order to account for differences in solution conditions. In 0.05 M citrate/0.1 M phosphate buffer, we find $pK_{eff} = 4.33$ for metMb (circles) and $pK_{eff} = 4.32$ for deoxyMb. For metMb, the titration curve shifts to lower pH in a buffer of reduced ionic strength (0.005 M citrate/0.01 M phosphate), yielding $pK_{eff} = 3.82$ (squares). In the transition region (pH 4.0–4.5), the observed absorption spectra change slowly with time and may take over an hour to reach equilibrium. The titration curves in Figure 1 are all based on the final steady-state spectra. Concurrent with these changes in the heme absorption, a 2-fold loss of intensity is observed in the peptide CD band of metMb at 220 nm (Irace et al., 1986; Morikis, 1990), indicating that the observed changes at the heme site are correlated with a conformational change of the polypeptide. Similar absorption and CD observations have been reported previously for metMb (Irace et al., 1986; Privalov et al., 1986; Acampora & Hermans, 1967) and interpreted (Irace et al., 1986) as being due to a conformational change of the polypeptide associated with a 50% loss of α-helical content.

In order to characterize more fully the perturbation of the

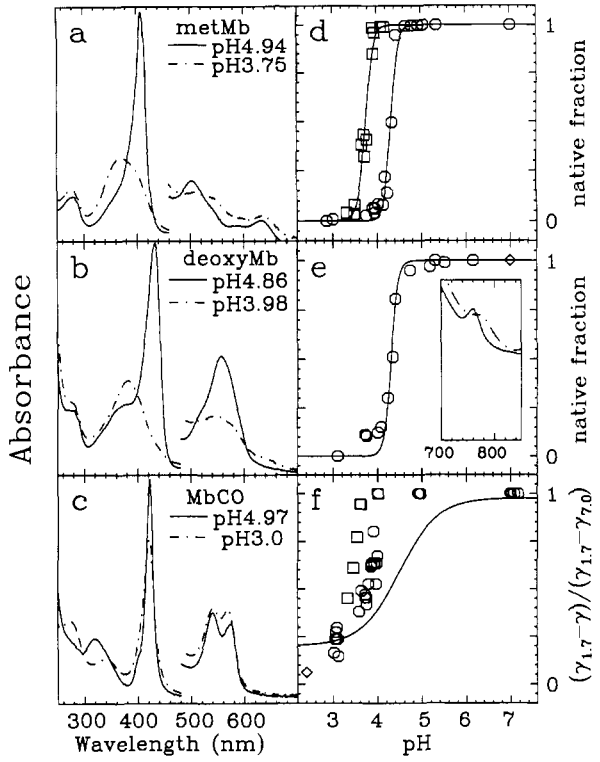

FIGURE 1: Effect of acid-induced partial unfolding on the absorption spectra of metMb (a and d), deoxyMb (b and e), and MbCO (c and f). The left-hand panels (a–c) show the observed spectra above (solid curve) and below (dashed curve) the conformational transition. The inset in (e) shows near-IR spectra recorded on deoxyMb samples separate from those shown in (b). For metMb and deoxyMb, spectra at intermediate pH are simple superpositions of spectra at the high and low pH extremes, and the right-hand panels (d and e) show the fractional contribution to the strong Soret absorption band due to native protein as a function of pH. The solid lines in panels d and e are the results of a fit using eq A.3 and the parameters given in the text. For MbCO, the change in the absorption spectrum upon lowering the pH is less dramatic, and the quantity plotted in the right-hand panel (f) thus shows the variation of the full width at half-maximum relative to extreme values taken at pH 7.0 and 1.7. For comparison with the sharp transitions shown in panels d and e, the solid line in (f) shows the fractional population of the closed conformation reported previously for MbCO (Morikis et al., 1989). The near-IR absorption spectra shown in (e) refer to samples at pH 5.70 (solid curve) and 3.27 (dashed line). The deoxyMb spectra shown in (b) and titration points marked with diamonds are measurements in 0.1 M phosphate buffer, and the titration points marked with squares in (d) were measured in 0.005 M citrate/0.01 M phosphate buffer. All other data in the figure refer to measurements on samples in 0.05 M citrate/0.1 M phosphate buffer.

heme site in response to the protein conformational change, we turn to RR spectroscopy. Due to the large blue shift of the Soret absorption band at low pH, it is difficult to obtain high-quality RR spectra of the low-pH forms of metMb or deoxyMb by using excitation near resonance with the Soret band of the neutral pH species (see Figure 2d), and we have thus chosen to make spectral comparisons by using 363.8-nm excitation (Figure 2a,b). Below pH 4, the RR spectrum of deoxyMb reveals frequency changes in several vibrational modes commonly used as indicators of iron oxidation and spin states, which shift from values (ν_4 = 1356 cm^{-1}, ν_3 = 1473 cm^{-1}) characteristic of high-spin ferrous heme to values (ν_4 = 1372 cm^{-1}, ν_3 = 1503 cm^{-1}) most often reported for low-spin ferric hemes. We observe no further changes in the deoxyMb RR spectrum down to pH 2.6. This low pH form of deoxyMb is nevertheless reduced, as addition of CO to the solution results in conversion to a species with absorption (not shown) and Raman (Figure 2e) spectra identical with those we observe

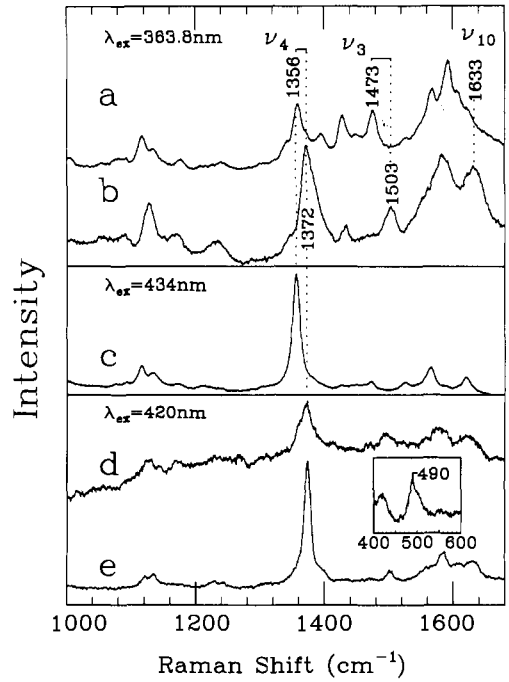

FIGURE 2: Traces a–d are resonance Raman spectra of deoxyMb above (a, pH 5.05; c, pH 5.0) and below (b, pH 3.92; d, pH 3.59) the acid-induced conformational transition apparent in the absorption spectra. Resonance enhancement of deoxyMb with blue excitation (c, λ_{ex} = 434 nm; d, λ_{ex} = 420 nm) decreases dramatically below pH 4 due to the large shift of the Soret band; thus it is more convenient to make spectral comparisons by using higher frequency excitation (a and b, λ_{ex} = 363.8 nm). The shift of ν_4 from 1356 to 1372 cm^{-1} and ν_3 from 1473 to 1503 cm^{-1} indicates breakage of the bond between iron and proximal histidine, leading to a four-coordinate, intermediate-spin ferrous heme. Although values in this range are also seen for low-spin ferric hemes, the iron is clearly reduced in trace d, as addition of CO to the same sample generates the spectrum of MbCO shown in trace e (λ_{ex} = 420 nm), including the Fe–CO stretching mode observed at 490 cm^{-1} (shown in inset). The samples of traces a–c are in 0.1 M citrate/0.2 M phosphate buffer; 0.05 M citrate/0.1 M phosphate buffer was used for the sample of traces d and e. Laser powers and integration times were (a) 50 mW, 1200 s; (b) 50 mW, 1200 s; (c) 30 mW, 300 s; (d) 5 mW, 1000 s; and (e) 5 mW, 200 s (main trace) or 400 s (inset).

for MbCO at acid pH. The observed values of the porphyrin vibrational frequencies (Figure 2b) are in fact consistent with those observed for four-coordinate, intermediate-spin ferrous hemes (Andersson et al., 1989; Sibbett et al., 1986; Nagai et al., 1980a; Kitagawa & Teraoka, 1979; Spiro & Burke, 1976), indicating that the proximal histidine no longer binds to the heme in the low-pH deoxy state. The broad peak at 1633 cm^{-1} probably contains contributions from both the vinyl stretching mode, observed at 1620 cm^{-1} in deoxyMb at pH 7, and the depolarized mode, ν_{10}, which is expected to occur in the range 1637–1642 cm^{-1} for a four-coordinate heme (Andersson et al., 1989). A similar overlap occurs in MbCO at low pH (see below). The breakage of the iron–histidine bond should be accompanied by the disappearance of the iron–histidine stretching mode located at 220 cm^{-1} in native deoxyMb; however, we were unable to confirm this directly as a large Rayleigh scattering background obscured the low-frequency region of the Raman spectrum.

A comparison of resonance Raman spectra of metMb above and below the acid-induced conformational transition also reveals changes in modes sensitive to axial coordination (Figure 3a,b). In particular, the ν_3 mode shifts from 1482 cm^{-1} at neutral pH to 1494 cm^{-1} at pH $\leq$ 4. These frequencies are in the ranges typically observed for six- and five-coordinate high-spin ferric hemes, respectively, indicating that the con-

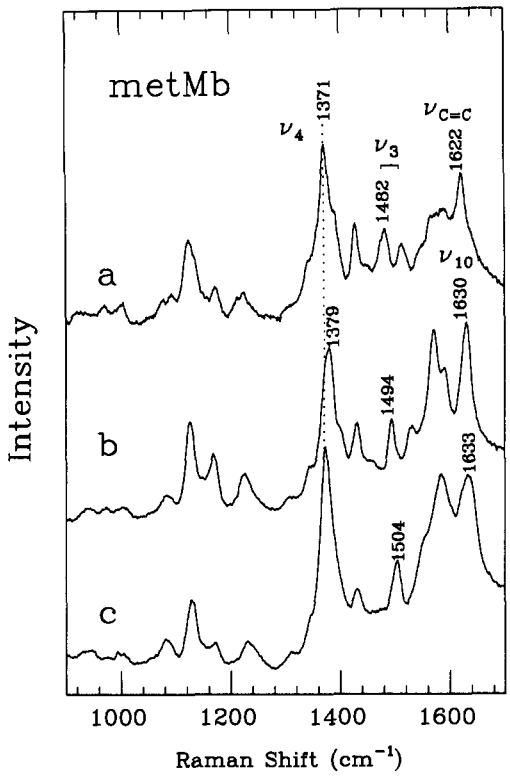

FIGURE 3: Resonance Raman spectra of metMb at pH 4.97 (a) and at pH 3.75 (b) and of photoreduced Mb at pH 3.75 (c). The shift of the ν_3 mode from 1482 to 1494 cm^{-1} demonstrates a reduced coordination number for the heme iron in the low-pH form of metMb. The spectrum in (c) was recorded by using the same sample as in (b) after thorough flushing with dry Ar gas to remove oxygen. All samples are in 0.1 M citrate/0.2 M phosphate buffer. All spectra were recorded by using 363.8-nm excitation. Laser powers and integration times were (a) 44 mW, 800 s; (b) 30 mW, 1800 s; and (c) 90 mW, 1200 s.

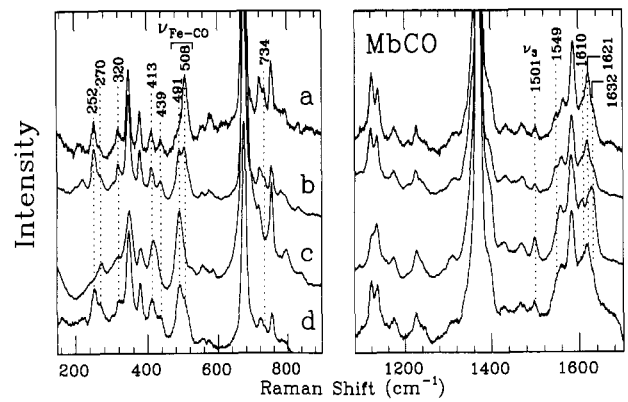

FIGURE 4: Resonance Raman spectra of MbCO at (a) pH 5.10, (b) pH 4.50, (c) pH 3.91, all in 0.1 M citrate/0.2 M phosphate buffer, and at (d) pH 3.60, in reduced ionic strength (0.005 M citrate/0.01 M phosphate) buffer. Modes at 252, 320, 439, and 734 cm^{-1} disappear or lose intensity as the pH is lowered below 4 but can be partially restored by reducing the ionic strength (d), suggesting that the spectral changes are coupled to the N → U transition. Scattering was excited from MbCO in a spinning cell in order to minimize CO photolysis in the scattering volume and all spectra were recorded with λ_{ex} = 420 nm. Laser powers and integration times for high and low frequency ranges, respectively, were (a) 5 mW, 200 and 500 s; (b) 30 mW, 600 and 900 s; (c) 22 mW, 300 and 600 s; and (d) 65 mW, 600 and 800 s.

formational transition is coupled with the loss of an axial ligand in metMb as well as deoxyMb. This coordination change is confirmed by the appearance of a depolarized mode ($\rho \simeq 0.6$) in the low-pH spectrum at a frequency (1630 cm^{-1}) typical of ν_{10} for five-coordinate hemes (Teraoka & Kitagawa, 1980). The large blue shift of the Soret band at low pH suggests that, as in deoxyMb, the proximal histidine is the ligand lost in metMb. The ν_4 mode is expected to occur at approximately the same frequency for either a six- or five-coordinate ferric heme but is not clearly visible in the RR spectrum of metMb at low pH. Note that the peak observed at 1379 cm^{-1} has a substantial depolarized component ($\rho \simeq 0.4$) and is probably a composite of more than one mode, precluding a definitive assignment of ν_4. As for deoxyMb, we were unable to directly observe the presence or absence of the iron–histidine stretching mode located at 248 cm^{-1} in native metMb (Kitagawa & Teraoka, 1981) due to a large Rayleigh scattering background at low frequencies. A final interesting observation is that irradiation of a thoroughly deoxygenated sample of metMb at pH ≤ 4 with a tightly focused 90-mW beam produces a RR spectrum (Figure 3c) identical with that observed for deoxyMb at low pH (Figure 2b), indicating that the heme is being photoreduced to a four-coordinate state.

MbCO. With CO bound to the heme, the observed changes in optical absorption upon going to acid solution are much less pronounced (see Figure 1c,f). The Soret band broadens noticeably, but the peak shifts only minimally from 422.5 nm (at neutral pH) to 421.5 nm (for pH ≤ 4). In spite of the less dramatic absorption changes, the peptide CD band at 222 nm in MbCO shows a 2-fold intensity loss similar to that seen for metMb (Morikis, 1990), indicating that CO binding does not substantially inhibit the global conformational changes that take place at low pH. The conformational change, however, does not produce the strong electronic perturbation of the heme observed for metMb and deoxyMb. In particular, there is no large shift of the Soret band, as would be expected on the basis of model compound studies (Traylor et al., 1985; Rougee & Brault, 1973, 1975), if the proximal histidine were lost. Since we cannot cleanly deconvolve spectral contributions due to the native and partially unfolded species, we simply plot the change in Soret line width as a function of pH in Figure 1f. The boxes and circles in Figure 1f again refer to buffer concentration and show a smaller ionic strength effect than in metMb.

A previous study from this laboratory characterized the pH-dependent equilibrium between open and closed conformational substates of the native protein (Morikis et al., 1989) by using the Fe–CO stretching frequencies observed in RR as a probe of the structure of the distal heme pocket in MbCO. At neutral pH, the A_1 CO conformer (ν_{Fe-CO} = 508 cm^{-1}) associated with the closed protein conformation is predominantly populated (Figure 4a), but upon lowering the pH to 4.5, the A_0 band (ν_{Fe-CO} = 491 cm^{-1}) associated with the open conformation acquires an area comparable to that of the A_1 band (Figure 4b). When the pH is reduced below 4, additional spectral changes occur. In particular, vibrational modes located at 252, 320, 439, 734, and 1549 cm^{-1} either lose intensity or disappear completely, while a mode at 1610 cm^{-1} gains intensity (Figure 4c). The vinyl stretching mode, located at 1621 cm^{-1} at neutral pH, appears to shift to higher frequency at low pH, but polarization measurements (not shown) indicate that this apparent shift is due to the growth in intensity of a depolarized mode at ~1632 cm^{-1}, which we assign as ν_{10}. The mode located at 413 cm^{-1} at neutral pH broadens and shifts to 417 cm^{-1} below pH 4. Lowering the ionic strength of the solution, which we have shown to shift the midpoint of the transition to lower pH in metMb (Figure 1d), largely reverses all of the intensity changes observed in the RR spectrum upon acidification (Figure 4d).

The presence or absence of the iron–histidine bond is a key issue that is not easily resolved, since the iron–histidine

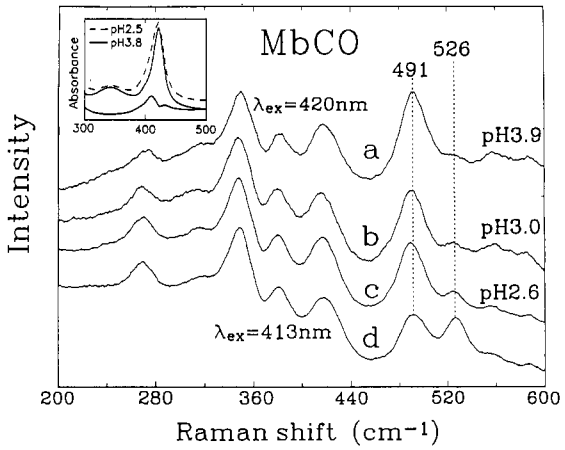

FIGURE 5: Low-frequency resonance Raman spectrum of MbCO in the U state as a function of pH and excitation wavelength. Spectra excited at 420 nm, near the Soret maximum, contain a weak peak at 526 cm^{-1} whose intensity progressively increases in samples at (a) pH 3.91, (b) pH 3.04, and (c) pH 2.63. Comparison of spectra recorded for the pH 2.63 sample by using (c) 420-nm and (d) 413-nm excitation demonstrates a marked increase in the intensity of the 526-cm^{-1} peak at the expense of the 491-cm^{-1} peak upon blue-shifting the excitation wavelength. As shown in the inset, the blue edge of the Soret band also broadens slightly as the pH is lowered from 3.8 to 2.5. A weak absorption peak near 410 nm is observed when the pH 3.8 spectrum is subtracted from the pH 2.5 spectrum with a weight chosen to approximately cancel the N band at 342 nm (inset, lower solid curve). All Raman data were gathered from MbCO samples in rapidly spinning cells; laser powers and integration times were (a) 22 mW, 300 s; (b) 12 mW, 1500 s; (c) 29 mW, 1200 s; and (d) 20 mW, 1800 s.

stretching mode has not yet been identified in the RR spectrum of MbCO. However, the Fe–CO stretching frequency is known to be sensitive to the presence and nature of the trans ligand (Yu & Kerr, 1988), and observations of the Fe–CO stretching region of the RR spectrum can thus provide evidence on the proximal ligation state. The 490-cm^{-1} peak that first appears above pH 4 persists following the N → U transition (Figure 4), indicating continued histidine ligation in the U state. However, a more careful observation of this region also reveals a weak peak at 526 cm^{-1}, which appears below pH 4 and increases in intensity as the pH is lowered further (Figure 5). Shifting the excitation wavelength from 420 to 413 nm leads to substantial enhancement of the 526-cm^{-1} mode relative to the 490-cm^{-1} mode, suggesting that this mode corresponds to a species with a blue-shifted Soret band. The blue edge of the Soret band also broadens slightly as the pH is lowered (see inset to Figure 5). When absorption spectra recorded at pH 3.8 and 2.6 are weighted to give approximately equal absorbances in the N band at 342 nm, the difference spectrum contains a weak peak at 410 nm. Together, these observations indicate the presence of a minority MbCO species with a strengthened Fe–CO bond and a Soret peak near 410 nm.

Cross-Section Measurements. As an aid to interpreting the Raman photolysis data presented in the following paper (Sage et al., 1990), we also present measurements of scattering cross sections for the ν_4 mode at several wavelengths (Table I). At neutral pH, scattering intensities of both the ν_4 mode and the 981-cm^{-1} mode of sulfate were measured for deoxyMb (Bangcharoenpaurpong et al., 1984) and MbCO (Morikis et al., 1991) in solutions containing 1.0 M sulfate. Cross sections were then calculated from the relative intensities of the two peaks, the relative concentrations of protein and sulfate, and the known (Schomacker et al., 1986) cross section of sulfate. For pH ≤ 4, MbCO precipitates in the presence of such high sulfate concentrations, and cross sections could not be obtained in this way. For MbCO at low pH, therefore, we measured the band area of ν_4 relative to the water OH stretching band at ~3300 cm^{-1}, rather than to the sulfate band, and determined the absolute cross section of the water band in an independent measurement on a sample of 1.0 M sulfate in water. The cross section of the low-pH deoxyMb species at 420 nm was estimated by a direct comparison of the absolute ν_4 peak intensities in Figure 2d,e. The results of these measurements, summarized in Table I, show that the scattering cross section of the MbCO ν_4 mode is reduced at low pH, as might be expected on the basis of changes in the Soret absorption band (Figure 1c). With blue excitation ($\lambda_{ex} \geq 420$ nm), where the Raman photolysis measurements presented in the following paper (Sage et al., 1991) were conducted, Table I shows that the cross section of MbCO below pH 4 is comparable to that expected for a five-coordinate deoxyMb species (pH 7), whereas the cross section of the four-coordinate deoxyMb species that we observe at pH 4 is more than an order of magnitude smaller. This observation is important for the dynamical analysis presented in the following paper (Sage et al., 1991).

Table I: Absolute Raman Scattering Cross Sections of ν_4 Modes of Myoglobin

	vibrational frequency (cm^{-1})	cross section ($\times 10^{24}$)[a] 420 nm[b]	427 nm[b]	434 nm[b]	441 nm[b]
MbCO, pH 7[c]	1374	6.9	4.3	0.99	0.32
MbCO, pH 3.91[d]	1374	4.8	3.4	1.9	1.3
deoxyMb, pH 7[e]	1356	3.7	3.1	2.8	1.8
deoxyMb, pH 4[d]	1372	~0.2			

[a] Absolute differential scattering cross sections for 90° scattering geometry. Units: cm^2/(steradian-molecule). [b] Excitation wavelength. [c] Morikis et al. (1991). [d] This work. [e] Bangcharoenpaurpong et al. (1984).

Discussion

Global Structure at Low pH. Characterization of the U state has potential interest in the understanding of Mb folding. Although early studies (Breslow & Gurd, 1962; Acampora & Hermans, 1967) treated the U state as completely unfolded, more recent work shows that the acid conformation is distinct both thermodynamically and spectroscopically from the fully unfolded, random-coil configuration (Bismuto et al., 1983; Irace et al., 1986). The U state of myoglobin retains approximately 50% of the α-helical structure of the native conformation (Bismuto et al., 1983). Tryptophan and tyrosine residues are less exposed to solvent in apomyoglobin at low pH than in the fully unfolded protein produced by exposure to high concentrations of guanidine hydrochloride. These results suggest that the U state may be a stable intermediate on the myoglobin unfolding pathway (Irace et al., 1986).

It has long been known that the U state in metMb is correlated with a blue-shifted Soret band (Breslow & Gurd, 1962), and this fact allows a convenient spectroscopic titration of the N ⇌ U equilibrium in the oxidized state (Acampora & Hermans, 1967; Puett, 1973). Our optical titration of metMb is consistent with previous work and is repeated here primarily for comparison with deoxyMb and MbCO. The sharp transition in the range pH 4.0–4.5 is well described by using the parameters reported by Puett (1973), if pK_{eff} is allowed to vary with solution ionic strength. The ionic strength dependence has been observed previously (Friend & Gurd, 1979) and is most likely due to stabilization of the fully protonated U state caused by screening of electrostatic interactions. In terms of our simple model (see Appendix), an in-

crease in ionic strength causes a decrease in K_n (and K_U) and a consequent increase in pK_{eff} (see eq A.4), consistent with observations.

We have shown that the deoxyMb absorption spectrum undergoes significant changes quite similar to those observed for metMb at low pH, and we suggest that both metMb and deoxyMb undergo a change in global conformation at low pH that leads to rupture of the iron–histidine bond. The Soret band of MbCO does not exhibit such dramatic changes upon lowering the pH. We nevertheless infer that a similar global conformation change occurs here as well, on the basis of changes in the peptide CD band similar to those observed for metMb. This conclusion is supported by the observation of changes in the RR spectrum of MbCO, which shows an ionic-strength-dependent transition near pH 4, as monitored, for instance, by the loss of the 252-cm^{-1} mode (see Figure 4). However, the lack of a dramatic change in the absorption spectrum along with transient Raman studies that probe proximal ligation subsequent to CO photolysis (Sage et al., 1991) suggests that MbCO remains six-coordinate in the U state.

It is important to realize that the N → U transition occurs due to protonation of all of the buried histidines (Breslow & Gurd, 1962; Puett, 1973) and thus is relatively insensitive to perturbations at the heme iron. For instance, reduction of the iron might be expected to increase the effective pK of the proximal histidine by weakening the iron–histidine bond, but the effect on the transition midpoint will be small since the observed pK_{eff} must represent the average behavior of all sites. Since we observe no significant shift in the transition midpoint upon reduction, the slight increase in pK_N is probably balanced by a slight increase in K_n (see eq A.4), due to the reduced positive charge on the protein. The results presented here also indicate that a conformational transition occurs even for MbCO, in which the proximal histidine remains bound to the majority of the hemes in the U state (see below) and only five sites contribute to the titration.

Heme Environment: MetMb and DeoxyMb. The RR spectra indicate that both metMb and deoxyMb have lost an axial ligand at low pH, concurrent with dramatic changes in the absorption spectra. Since the proximal histidine is the only axial ligand in deoxyMb, we conclude that the iron–histidine bond breaks at low pH. In metMb, the RR results do not give a direct indication of which ligand has been displaced, but the large change in electronic structure indicated by the absorption spectrum is unlikely to be due to displacement of the relatively weak field aquo ligand bound trans to the histidine. Thus, our data strongly suggest that breakage of the iron–histidine bond also takes place in metMb below pH 4. This conclusion is consistent with careful optical titration studies of metMb, which show that all of the histidine imidazole residues that are inaccessible to solvent in the native form become protonated during the acid-induced conformational change (Puett, 1973).

Although it is sometimes believed that the transition to the U state results in the loss of the heme, our results indicate that heme remains associated with the globin in spite of the loss of the iron–histidine linkage. We observe a four-coordinate heme down to pH 2.6, whereas reduced heme in aqueous solution coordinates with water molecules and usually aggregates. The absorption spectrum that we observe for deoxyMb at low pH is also distinct from that reported for reduced heme in aqueous solution (Antonini & Brunori, 1971). Significantly, addition of CO to the U state of deoxyMb results in a species that is spectroscopically indistinguishable from that formed when the pH of an MbCO solution is lowered, indicating that the proximal histidine remains close enough to rebind to the heme. To our knowledge, this is the first time that clear evidence has been reported for a protein-associated four-coordinate ferrous heme, although rupture of the protein linkage has been reported for the hemes in the α subunits of ferrous nitrosyl hemoglobin (Maxwell & Caughey, 1976; Perutz et al., 1976; Nagai et al., 1980b) in the presence of inositol hexaphosphate, and nickel porphyrins incorporated into hemoglobin are four-coordinate in half of the sites (Shelnutt et al., 1986).

Heme Environment: MbCO. In contrast to the large absorption changes seen upon lowering the pH in metMb and deoxyMb, the spectrum of MbCO changes only minimally in acid solutions, although CD measurements (Morikis, 1990) indicate a similar change in global conformation. On the basis of the reported absorption spectra for five- and six-coordinate carbonyl hemes (Traylor et al., 1985; Rougee & Brault, 1973, 1975) loss of the histidine ligand would be expected to result in a 20–25-nm blue shift of the Soret band. The Raman data also fail to show the changes expected upon complete rupture of the iron–histidine linkage. In particular, the stretching frequency of the iron–carbon bond is 25–30 cm^{-1} higher for model hemes without a sixth ligand than for those with nitrogenous bases such as imidazole bound trans to the CO (Yu & Kerr, 1988). The persistence of a strong 490-cm^{-1} mode is thus clear evidence for dominant histidine ligation at low pH. This conclusion is corroborated by the presence of the iron–histidine stretching mode in the RR spectrum of the low-pH MbCO photoproduct (Sage et al., 1991). The existence of an intact iron–histidine bond in MbCO following a rapid pH drop has been noted previously (Han et al., 1990); the present results show that this bond remains dominant in equilibrium.

However, the results presented above indicate the presence of an additional MbCO species with a strengthened Fe–CO bond and blue-shifted Soret band. Although the Fe–CO stretching frequency (ν_{Fe-CO} = 526 cm^{-1}) is similar to that observed in the absence of a trans ligand (Yu & Kerr, 1988), there is no indication of an absorption feature near 395 nm, where the Soret maximum is expected for a five-coordinate CO-bound heme. The data thus suggest that the 526-cm^{-1} mode corresponds to a species in which the proximal histidine has been replaced by a weak ligand. Since Fe–CO frequencies in the 520–530-cm^{-1} range are also observed with weak ligands bound trans to CO (Yu & Kerr, 1988) and reported absorption data for protoheme with CO and H_2O as axial ligands (Wang & Brinigar, 1979) indicate a Soret maximum at 406.5 nm in aqueous solution, our observations are consistent with replacement of the proximal histidine with a water ligand in a minority fraction of the proteins. The present data do not allow us to definitively exclude other candidates for the new ligand. We note, however, that replacement of the histidine ligand with a solvent-derived water molecule has been suggested previously for a transient deoxyMb species observed following a rapid pH drop (Han et al., 1990).

It would be of some interest to quantify the relative populations of the two observed MbCO species. Unfortunately, the Fe–CO band intensities are not reliable population measures since the Raman scattering cross sections for the two species are not known. In particular, the observed intensity ratio varies significantly with excitation wavelength (Figure 5c,d) due to maximal enhancement of the Fe–CO bands in resonance with the corresponding Soret excitations, and the intensity ratio observed at a particular wavelength can thus

be quite misleading. The Franck–Condon coupling of the Fe–CO mode to the Soret excitation may also be affected by the replacement of the trans ligand. However, the peak of the composite Soret band shifts only 1 nm upon the N → U transition and the feature near 410 nm is only apparent in the difference spectrum. This suggests that the feature at 410 nm and the 526-cm^{-1} band correspond to a minority MbCO species even at pH 2.6. Thus, although the proximal ligation equilibrium is perturbed in the U state, histidine ligation remains dominant in MbCO.

Intensity changes noted for several other modes in the MbCO RR spectrum provide spectroscopic markers of structural alterations of the heme environment below pH 4. Since the modes in question have not been assigned for MbCO, a specific interpretation of these changes is difficult. The mode at 439 cm^{-1} in the MbCO spectrum, for instance, may be analogous to a mode appearing at 441 cm^{-1} in deoxyMb and assigned to pyrrole folding (Choi & Spiro, 1983), but an explanation for the intensity change is not obvious. We speculate that some loosening of the heme pocket occurs due to the acid-induced conformational change and that the reduced strain on the heme lessens deviations from D_{4h} symmetry that allow some out-of-plane modes to become enhanced in the native protein environment (Choi & Spiro, 1983). On the basis of the fact that the 252-cm^{-1} mode disappears in Mb mutants where the proximal histidine is replaced with tyrosine (Egeberg et al., 1990), one might infer that this mode is due to iron–histidine stretching. However, the mode loses intensity at low pH in MbCO, where the majority of the iron–histidine bonds remain intact, as discussed above. In fact, isotropic labeling studies indicate that the 252-cm^{-1} mode is not due to stretching of the iron–histidine bond (A. V. Wells, D. M. Morikis, J. T. Sage, P. M. Champion, M. Chiu, and S. G. Sligar, manuscript in preparation), and its coupling to the Soret transition must therefore be sensitive to other changes in the heme environment.

Comparison: A_1/A_0 vs N/U. It is appropriate to comment here on the relation of the present spectroscopic characterization of the partially unfolded U state to the previous study (Morikis et al., 1989) of the open protein conformation associated with the A_0 CO conformer. We particularly want to stress several unambiguous distinctions between the U state characterized here and the open conformation studied previously.

(1) On the basis of changes in the intensity of the peptide CD band (Puett, 1973; Irace et al., 1986; Morikis, 1990), the N → U transition clearly involves a global change in protein conformation accompanied by a substantial loss of α-helical content. In contrast, transition to the open conformation is believed to be a local event, primarily involving a displacement of Arg-CD3 that allows freer motion of the distal histidine and imparts greater flexibility to the distal heme pocket (Lecomte & La Mar, 1985; Kuriyan et al., 1986).

(2) The transition to the U state is known to be a cooperative event driven by the protonation of six histidine residues that are not accessible to solvent in the native conformation (Breslow & Gurd, 1962; Puett, 1973). The free energy of the open conformation is also influenced by pH, but only a single protonation site is involved, probably the distal histidine (Morikis et al., 1989). This difference is quite apparent from the titration curves: although the midpoint occurs in the range pH 4.0–4.5 for both the A_0/A_1 and N/U titrations, the latter curve (n = 6) exhibits a very sharp transition (Figure 1d,e) relative to the former (n = 1; Morikis et al., 1989; see solid curve, Figure 1f).

(3) The A_0 band is observed in MbCO crystals near neutral pH (Makinen et al., 1979; Morikis et al., 1988), yet the presence of a substantial fraction of protein in the U state is clearly incompatible with the observed high-resolution X-ray structure (Kuriyan et al., 1986). Moreover, the $A_0 \rightleftarrows A_1$ equilibrium can be substantially altered in crystals by changing the pH (Morikis, 1990), while the N ⇄ U transition ought to be severely hindered in the crystal environment.

(4) The interconversion time scales of the N ↔ U and A_0 ↔ A_1 equilibria differ drastically. At pH 4.33, more than an hour is required to establish steady-state populations of N and U in deoxyMb, while at pH 4.4 interconversion between the states associated with A_0 and A_1 occurs rapidly compared to the millisecond CO binding time scale (Lecomte & La Mar, 1985; Morikis, 1990).

(5) Finally, on the basis of measurements of the free energy of stabilization of sperm whale myoglobin at neutral pH (Puett, 1973; Acampora & Hermans, 1967), the population of the U state at neutral pH is expected to be negligible. In contrast, there is ~3% population of the A_0 state at neutral pH (Shimada & Caughey, 1982; Ansari et al., 1987; Morikis et al., 1989).

On the basis of these observations, we conclude that changes observed above pH 4.5 in the Fe–C and C–O stretching regions of RR and IR spectra (Morikis et al., 1989; Ansari et al., 1987) are not associated with partial unfolding of the protein (transition to the U state). The present results are thus consistent with the previous description (Morikis et al., 1989), in which the A_0 CO conformer was correlated with the open distal pocket conformation proposed on the basis of X-ray diffraction studies of MbCO crystals (Kuriyan et al., 1986) and solution NMR investigations (Lecomte & La Mar, 1985).

An interesting possibility suggested by points 4 and 5 above is that the open state may have a functional role at room temperature, in spite of its relatively low population. Since the open and closed conformations are in relatively fast exchange at room temperature, the kinetics of the system are described by average rates weighted by the populations of the two states. Exchange between the closed and open conformations is expected to transiently open a potential pathway for ligand migration between the heme pocket and the solvent (Kuriyan et al., 1986), and may affect the orders of magnitude of the rates at which CO enters and leaves the pocket. The relative magnitudes of the exit and geminate rebinding rates play a key functional role in determining whether the overall second-order binding rate is controlled by the rate of entry to the heme pocket or the rate of binding to the heme.

A proper evaluation of the role of the open conformation in room-temperature kinetics will require much deeper experimental investigation. A complete picture must include not only the relative populations of the open and closed conformations but also the rates appearing in the kinetic model for each of these conformations. The situation is complicated considerably by the fact that the bound ligand interacts with the distal pocket so that the relative populations of the open and closed conformations in deoxyMb are not necessarily the same as those observed with CO bound.

It is also important to note that, even at pH 3.15, there remains a significant (~12%) population of the A_1 CO conformation that gives rise to the Fe–CO peak observed at 508 cm^{-1} (Morikis et al., 1989). Since this peak has been attributed to a state in which the CO is prevented from binding in the energetically favorable upright position with respect to the heme due to steric hindrance from the distal heme pocket (Fuschsman & Appleby, 1979), this observation strongly

suggests that the distal heme pocket retains significant structural integrity following the N → U conformational change. In the absence of any steric interaction with the polypeptide, 100% population of the upright A_0 conformation of the CO (ν_{Fe-CO} = 491 cm^{-1}) would be expected. The presence of a partially intact heme pocket in the U state is supported by the observation that the heme remains associated with the protein in the absence of any axial ligation in deoxyMb.

The retention of an element of tertiary structure (the heme pocket) in the face of a substantial loss of secondary structure (α-helical content) is highly interesting and suggests that the primary disorganization of the secondary structure takes place in a region remote from the heme site. This is consistent with previous indications that the heme plays a significant role in directing globin folding and stabilizing the native conformation (Leutzinger & Beychok, 1981). Previous suggestions of heme pocket disorganization at low pH were based on indirect observations involving the dye 1-anilino-8-naphthalenesulfonate (ANS), which binds to the heme pocket of apomyoglobin at neutral pH. Solvent-induced quenching of ANS fluorescence as the pH is lowered was interpreted as dissociation of the protein–ANS complex, due to a structural change in the heme pocket (Colonna et al., 1982, Shen & Hermans, 1972). However, since the association constant of the heme with the globin is at least 6 orders of magnitude larger than that for ANS, at least in the native conformation (Antonini & Brunori, 1971), loss of ANS binding under given solution conditions cannot be taken to imply loss of heme under similar conditions.

Observations on Four-Coordinate Heme. The existence of a protein-bound heme without direct axial ligation obviously provides an opportunity to obtain novel information on the effect of the axial ligand on heme electronic structure and reactivity. The primary effect of the protein environment on the heme is likely to be due to the chemistry of the axial ligand, but there have been suggestions that protein interactions with peripheral substituents of the heme can influence properties such as redox potential or ligand-binding affinity (Warshel & Weiss, 1981; Reid et al., 1986). Here we note two significant observations in the absence of the bond to the proximal histidine: the presence of a near-IR absorption band and the occurrence of photoreduction.

Observations of heme absorption usually concentrate on the intense B (Soret) and Q (α–β) bands attributed to π–π^* transitions of the porphyrin moiety, and less attention has traditionally been given to weaker bands arising from porphyrin–iron charge transfer transitions. Such bands are in principle quite sensitive to perturbations in the vicinity of the iron, and a greater understanding of the nature of these bands could provide a very useful tool for spectroscopic studies of heme proteins (Makinen & Churg, 1983). The peak wavelength of the weak band found near 760 nm in deoxyMb and deoxyHb, for instance, is believed to correlate with the out-of-plane displacement of the iron and has been used as a probe of protein relaxation following ligand photolysis (Agmon, 1988; Sassaroli & Rousseau, 1987; Campbell et al., 1987; Cordone et al., 1986; Ansari et al., 1985). The 15-nm red shift that we observe on the breakage of the iron–histidine bond at low pH is qualitatively consistent with motion of the iron into the heme plane according to the proposed correlation. By using a linear approximation for the shift, $\Delta\lambda \simeq \alpha\Delta x$, with α = 8 nm/atomic unit (Agmon, 1988), the observed 15-nm red shift leads to $\Delta x \simeq 1$ Å, which is somewhat higher than the ~0.5-Å iron displacement expected upon the transition to a planar heme. Since the transition energy is likely to scale quadratically rather than linearly with the iron out-of-plane coordinate (Šrajer et al., 1986), the linear approximation used above leads to a numerical discrepancy that is accounted for when quadratic dependence is assumed (V. Šrajer and P. M. Champion, manuscript in preparation).

The absorption band at 760 nm has been assigned, on the basis of single-crystal absorption studies and the results of molecular orbital calculations, to a Fe $d_{x^2-y^2}$–porphyrin π^* transition (Makinen & Churg, 1983). However, the observation of the band in deoxyMb at low pH refutes such an assignment since the S = 1 ground state of a four-coordinate ferrous heme has a vacant $d_{x^2-y^2}$ orbital (Collman et al., 1976; Lang et al., 1978). Absorption measurements on four-coordinate heme model compounds also show a similar near-IR band (Brault & Rougee, 1974). Reasonable alternative assignments for this band can be restricted to transitions involving the iron d orbitals and the highest occupied (a_{1u}, a_{2u}) and lowest unoccupied (e_g) orbitals of the porphyrin. Since the band is known to be xy polarized (Makinen & Churg, 1983), only four assignments are possible in nominal D_{4h} symmetry: $a_{1u} \rightarrow d_\pi$, $a_{2u} \rightarrow d_\pi$, $d_{xy} \rightarrow e_g$, and $d_{z^2} \rightarrow e_g$. The latter assignment can also be ruled out, since the energy shift of the d_{z^2} orbital upon loss of the histidine ligand must be very much larger than that observed for the 760-nm band. We note that the assignment of the analogous near-IR band in deoxyhemoglobin to an $a_{2u} \rightarrow d_{yz}$ transition (Eaton et al., 1978) is consistent with these restrictions.

A correct assignment for the iron d orbital involved in this transition is important for two reasons. First, it would allow a more fundamental interpretation of sophisticated physical studies based on observations of this band. Second, variations of the band intensity with temperature (Cupane et al., 1988) may be due to thermal population of low-lying d orbitals, and an analysis of such temperature variations could yield important information on low-lying electronic states of the iron. The nature of the ground state of the high-spin ferrous iron has not been satisfactorily resolved on the basis of other spectroscopic studies [e.g., Kent et al. (1979)], and such information will be needed for the complete interpretation of studies that probe spin-dependent effects in ligand binding to the heme (Gerstmann et al., 1989).

A second interesting observation is that photoreduction of the heme iron occurs in metMb solution at low pH. We have previously investigated photoreduction in metMb crystals and found that the process appeared to be coupled to the Soret transition (Sage et al., 1989). (Recently, we have also succeeded in observing photoreduction in carefully deoxygenated solutions of metMb at neutral pH.) Studies on model compounds led to the contrary conclusion that photoreduction was driven by an iron–imidazole charge transfer transition (Ozaki et al., 1987), although the analysis of this data has been questioned (Sage et al., 1989). The present observation of photoreduction in the absence of an axial imidazole at low pH demonstrates that this ligand is not required for the photoreduction process in Mb. The observation of facile photoreduction in mutant myoglobins in which the distal aquo ligand is displaced (Morikis et al., 1990) indicates that neither axial ligand plays the role of electron donor in the photoreduction process. Detailed studies of this interesting photochemical process will be published elsewhere (Y. Gu, P. Li, J. T. Sage, and P. M. Champion, manuscript in preparation).

Conclusions

In the vicinity of pH 4, myoglobin undergoes a cooperative, ionic-strength-dependent conformational change that leads to a substantial loss of secondary structure. Using resonance

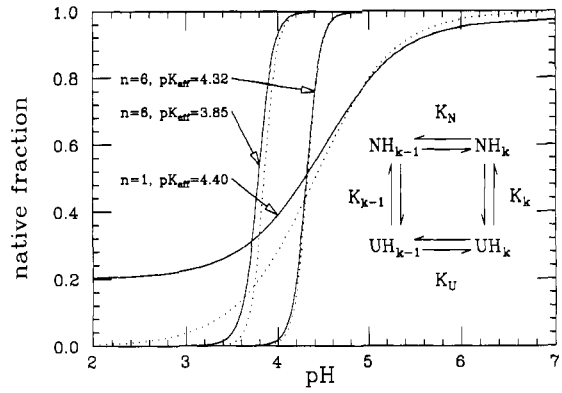

FIGURE 6: Fractional population of N state $[N/(N + U)]$ as a function of pH calculated by using either eq A.3 (solid lines) or the simplified expression obtained by dropping the second factor in eq A.3 (dotted lines). The coupled protonation/conformation scheme used in the derivation of eq A.3 is shown as an inset. Values of n and pK_{eff} used in calculating the curves are shown. For the $n = 6$ curves, the values $pK_N = 3.0$ and $pK_U = 5.9$ were used. The solid $n = 1$ curve is identical with that shown in Figure 1f and uses values $pK_N = 3.8$ and $pK_U = 6.0$.

Raman spectroscopy, we have carried out a detailed spectroscopic characterization of local changes at the heme site induced by this global conformational transition. Although similar global conformations are seen for different heme iron oxidation and ligation states, the structure of the immediate heme environment varies. Most significantly, the bond between the proximal histidine and the heme iron ruptures in both metMb and deoxyMb below pH 4, but the majority of these bonds reform when CO is bound. Despite a substantial change in the global structure of the protein, the heme pocket appears to remain at least partially intact, and it is likely that the loss of secondary structure occurs in a region not directly associated with the heme. The global conformational change studied here is clearly distinct from the local closed to open transition of MbCO studied earlier (Morikis et al., 1989). The present work suggests that resonance Raman spectroscopy may be useful for studying denaturation processes in other heme proteins, since it provides a more specific probe of the heme environment than visible absorption alone.

Further studies of myoglobin at low pH will provide an opportunity for understanding the spectroscopic and functional role played by the proximal ligand. For instance, observations of the four-coordinate heme associated with the U state of deoxyMb have revealed information relevant to an understanding of heme photoreduction and to assignment of the 760-nm charge transfer band. Of particular interest is the role played by the proximal histidine in the binding of exogenous ligands at low pH. The results presented here demonstrate that the iron–histidine bond is strongly stabilized by CO ligation. The complex kinetics governing the transition between the stable four- and six-coordinate states are explored in the following paper.

Added in Proof

While this paper was under review, a structural characterization of an acid-induced folding intermediate of apomyoglobin appeared (Hughson et al., 1990). The analysis of NMR proton exchange measurements suggests that the termini of the polypeptide chain (A, G, and H helices) form a relatively compact domain in the intermediate state, while the B–E helices are unfolded. (No information was available for the F helix.) It is likely that the holoprotein state denoted U in the present work has structural features in common with the I state of the apoprotein studied by Hughson et al., although binding of heme may lead to additional structure formation.

Acknowledgments

We thank Dr. Denis Rousseau for pointing out the presence of a minority MbCO species with $\nu_{Fe-CO} = 526$ cm^{-1} below pH 4.

Appendix

The model presented here expands on the coupled protonation/conformation model used previously (Morikis et al., 1989) to describe the effect of distal histidine protonation on distal pocket conformation. We comment on the range of validity of a simple Henderson–Hasselbalch expression.

We adopt a model where a number, n, of protonatable groups are inaccessible to solvent in the native conformation and thus have different proton association constants, $K_N = [H][NH_{k-1}]/[NH_k]$ and $K_U = [H][UH_{k-1}]/[UH_k]$, in the native ($K_N$) and partially unfolded (K_U) states, respectively. Furthermore, we make the simplifying assumption that these two constants have the same values at all n protonation sites (see Figure 6). In this scheme, NH_k (or UH_k) represents the native (or partially unfolded) state of the protein with k sites protonated. If we specify an equilibrium constant for the fully protonated system, $K_n = [NH_n]/[UH_n]$, it follows from the above simplifications that the equilibrium constant for a given protonation number is independent of which sites are protonated and is related to K_n by

$$\frac{K_k}{K_n} = \left(\frac{K_N}{K_U}\right)^{n-k} \tag{A.1}$$

By using the above simplifications and eq A.1, it is straightforward to show that

$$\frac{N}{U} \equiv \frac{\sum_{k=1}^{n} \binom{n}{k}[NH_k]}{\sum_{k=1}^{n} \binom{n}{k}[UH_k]} = K_n\left(\frac{1 + 10^{pH-pK_N}}{1 + 10^{pH-pK_U}}\right)^n \tag{A.2}$$

A somewhat more general expression allowing different K_N and K_U at different protonation sites has been given by Tanford (1970). Equation A.2 can be written in a more transparent form as

$$\frac{N}{U} = 10^{n(pH-pK_{eff})}\left(\frac{1 + 10^{pK_N-pH}}{1 + 10^{pH-pK_U}}\right)^n \tag{A.3}$$

if we make the definition

$$pK_{eff} = pK_N - \frac{1}{n}\log K_n \tag{A.4}$$

Using eq A.1 again, we can express the effective pK more symmetrically in terms of an average proton association constant and an average conformational equilibrium constant:

$$pK_{eff} = \frac{1}{2}(pK_N + pK_U) - \frac{1}{2n}\log K_0K_n \tag{A.5}$$

Under conditions such that $K_N \gg [H^+] \gg K_U$ (or $pK_N < pH < pK_U$), the second factor in eq A.3 is approximately unity and the expression takes a useful Henderson–Hasselbalch form, in which the complexities of the conformational equilibrium are concealed within a single phenomenological constant, pK_{eff}. Figure 6 shows the native fraction $[N/(N + U)]$ as a function of pH, calculated by using eq A.3 (solid curves) and by using the Henderson–Hasselbalch form (dotted curves), for three values of pK_{eff}. It is clear that the Henderson–

Hasselbalch form can deviate substantially from the more accurate expression outside a narrow range of pH. It is possible that such deviations account for nonintegral values of n sometimes encountered in fitting spectroscopic titration data to a Henderson–Hasselbalch form with variable n [e.g., Fuchsman and Appleby (1979)].

Registry No. CO, 630-08-0; histidine, 71-00-1; iron, 7439-89-6; heme, 14875-96-8.

REFERENCES

Acampora, G., & Hermans, J., Jr. (1967) *J. Am. Chem. Soc. 89*, 1543–1552.

Agmon, N. (1988) *Biochemistry 27*, 3507–3511.

Andersson, L. A., Mylrajan, M., Sullivan, E. P., Jr., & Strauss, S. H. (1989) *J. Biol. Chem. 32*, 19099–19102.

Ansari, A., Berendzen, J., Bowne, S. F., Frauenfelder, H., Iben, I. E. T., Sauke, T. B., Shyamsunder, E., & Young, R. D. (1985) *Proc. Natl. Acad. Sci. U.S.A. 82*, 5000.

Ansari, A., Berendzen, J., Braunstein, D., Cowen, B. R., Frauenfelder, H., Hong, M. K., Iben, I. E. T., Johnson, J. B., Ormos, P., Sauke, T. B., Scholl, R., Schulte, A., Steinbach, P. J., Vittitow, J., & Young, R. D. (1987) *Biophys. Chem. 26*, 337.

Antonini, E., & Brunori, M. (1971) *Hemoglobin and Myoglobin in Their Reactions with Ligands*, North-Holland, Amsterdam.

Austin, R. H., Beeson, K. W., Eisenstein, L., Frauenfelder, H., & Gunsalus, I. C. (1975) *Biochemistry 14*, 5355–5373.

Bangcharoenpaurpong, O., Schomacker, K. T., & Champion, P. M. (1984) *J. Am. Chem. Soc. 106*, 5688–5698.

Bismuto, E., Colonna, G., & Irace, G. (1983) *Biochemistry 22*, 4165–4170.

Brault, D., & Rougee, M. (1974) *Biochemistry 13*, 4598–4602.

Braunstein, D., Ansari, A., Berendzen, J., Cowen, B. R., Egeberg, K., Frauenfelder, H., Hong, M. K., Ormos, P., Sauke, T. B., Scholl, R., Schulte, A., Sligar, S. G., Springer, B. A., Steinbach, P. J., & Young, R. D. (1988) *Proc. Natl. Acad. Sci. U.S.A. 85*, 8497–8501.

Breslow, E., & Gurd, F. R. N. (1963) *J. Biol. Chem. 237*, 371–381.

Campbell, B. F., Chance, M. R., & Friedman, J. M. (1987) *Science 238*, 373.

Cannon, J., Geibel, J., Whipple, M., & Traylor, T. G. (1976) *J. Am. Chem. Soc. 98*, 3395–3396.

Champion, P. M. (1988) in *Proceedings of the International Symposium on Frontiers in Science*, American Institute of Physics Conference Proceedings No. 180 (Chan, S. S., & Debrunner, P. G., Eds.) pp 310–324, American Institute of Physics, New York.

Champion, P. M. (1990) in *Protein Structure and Engineering* (Jardetzky, O., Ed.) pp 347–354, Plenum, New York.

Choi, S., & Spiro, T. G. (1983) *J. Am. Chem. Soc. 105*, 3683–3692.

Coletta, M., Ascenzi, P., Traylor, T. G., & Brunori, M. (1985) *J. Biol. Cehm. 260*, 4151–4155.

Coletta, M., Ascenzi, P., & Brunori, M. (1988) *J. Biol. Chem. 263*, 18286–18289.

Collman, J. P., Hoard, J. L., Kim, N., Lang, G., & Reed, C. A. (1975) *J. Am. Chem. Soc. 97*, 2676–2681.

Colonna, G., Balestrieri, C., Bismuto, E., Servillo, L., & Irace, G. (1982) *Biochemistry 21*, 212–215.

Cordone, L., Cupane, A., Leone, M., & Vitrano, E. (1986) *Biophys. Chem. 24*, 259.

Cupane, A., Leone, M., Vitrano, E., & Cordone, L. (1988) *Biopolymers 27*, 1977–1997.

Eaton, W. A., Hanson, K. H., Stephens, P. J., Sutherland, J. C., & Dunn, J. B. R. (1978) *J. Am. Chem. Soc. 100*, 4991–5003.

Egeberg, K. D., Springer, B. A., Martinis, S. A., Sligar, S. G., Morikis, D. M., & Champion, P. M. (1990) *Biochemistry 29*, 9783–9791.

Friend, S. H., & Gurd, F. R. N. (1979) *Biochemistry 18*, 4612–4619.

Fuchsman, W. H., & Appleby, C. A. (1979) *Biochemistry 18*, 1309–1321.

Geibel, J., Chang, C. K., & Traylor, T. G. (1975) *J. Am. Chem. Soc. 98*, 5924–5926.

Gerstmann, B., Roberson, M., & Austin, R. (1989) *J. Opt. Soc. Am. B 6*, 1050–1057.

Giacometti, G. M., Traylor, T. G., Ascenzi, P., Brunori, M., & Antonini, E. (1977) *J. Biol. Chem. 252*, 7447–7448.

Giacometti, G. M., Ascenzi, P., Bolognesi, M., & Brunori, M. (1981) *J. Mol. Biol. 146*, 363–374.

Han, S. H., Rousseau, D. L., Giacometti, G., Brunori, M. (1990) *Proc. Natl. Acad. Sci. U.S.A. 87*, 205–209.

Hughson, F. M., Wright, P. E., & Baldwin, R. L. (1990) *Science 249*, 1544–1548.

Irace, G., Bismuto, E., Savy, F., & Colonna, G. (1986) *Arch. Biochem. Biophys. 244*, 459–469.

Kent, T. A., Spartalian, K., & Lang, G. (1979) *J. Chem. Phys. 71*, 4899–4908.

Kitagawa, T., & Teraoka, J. (1979) *Chem. Phys. Lett. 63*, 443–446.

Kuriyan, J., Wilz, S., Karplus, M., & Petsko, G. A. (1986) *J. Mol. Biol. 192*, 133–154.

Lang, G., Spartalian, K., Reed, C. A., & Collman, J. P. (1978) *J. Chem. Phys. 69*, 5424–5427.

Lecomte, J. T. J., & La Mar, G. N. (1985) *Biochemistry 24*, 7388–7395.

Leutzinger, Y., & Beychok, S. (1981) *Proc. Natl. Acad. Sci. U.S.A. 78*, 780–784.

Makinen, M. W., & Churg, A. K. (1983) in *Iron Porphyrins* (Lever, A. B. P., & Gray, H. B., Eds.) pp 141–235, Addison-Wesley, Reading, MA.

Makinen, M. W., Houtchens, R. A., & Caughey, W. S. (1979) *Proc. Natl. Acad. Sci. U.S.A. 76*, 6042.

Maxwell, J. C., & Caughey, W. S. (1976) *Biochemistry 15*, 388–396.

Morikis, D. (1990) Ph.D. Thesis, Northeastern University, Boston, MA.

Morikis, D., Sage, J. T., Rizos, A. K., & Champion, P. M. (1988) *J. Am. Chem. Soc. 110*, 3641–3642.

Morikis, D., Champion, P. M., Springer, B. A., & Sligar, S. G. (1989) *Biochemistry 28*, 4791–4800.

Morikis, D., Champion, P. M., Springer, B. A., Egeberg, K. D., & Sligar, S. G. (1990) *J. Biol. Chem. 265*, 12143–12145.

Morikis, D., Li, P., Bangcharoenpaurpong, O., Sage, J. T., & Champion, P. M. (1991) *J. Phys. Chem.* (in press).

Murray, L., Hofrichter, J., Henry, E., & Eaton, W. (1988) *Biophys. Chem. 29*, 63–76.

Nagai, K., Kitagawa, T., & Morimoto, H. (1980a) *J. Mol. Biol. 136*, 271–289.

Nagai, K., Welborn, C., Dolphin, D., & Kitagawa, T. (1980b) *Biochemistry 19*, 4755–4761.

Nagai, K., Luisi, B., Shih, D., Miyazaki, G., Imai, K., Poyart, C., De Young, A., Kwiatkowski, L., Noble, R. W., Lin, S.-H., & Yu, N.-T. (1987) *Nature 329*, 858.

Olson, J. S., Mathews, A. J., Rohlfs, R. J., Springer, B. A., Egeberg, K. D., Sligar, S. G., Tame, J., Renaud, J.-P., &

Nagai, K. (1989) *Nature 336*, 265–266.
Ozaki, Y., Iriyama, K., Ogoshi, H., & Kitagawa, T. (1987) *J. Am. Chem. Soc. 109*, 5583–5586.
Perutz, M. F., Kilmartin, J. V., Nagai, K., Szabo, A., & Simon, S. R. (1976) *Biochemistry 15*, 378–387.
Privalov, P. L., Griko, Yu. V., Venyaminov, S. Yu., & Kutyshenko, V. P. (1986) *J. Mol. Biol. 190*, 487–498.
Puett, D. (1973) *J. Biol. Chem. 248*, 4623–4634.
Reid, L. S., Lim, A. R., & Mauk, A. G. (1986) *J. Am. Chem. Soc. 108*, 8197–8201.
Ringe, D., Petsko, G. A., Kerr, D. E., & Ortiz de Montellano, P. R. (1984) *Biochemistry 23*, 2–4.
Rougee, M., & Brault, D. (1973) *Biochem. Biophys. Res. Commun. 55*, 1364.
Rougee, M., & Brault, D. (1975) *Biochemistry 14*, 4100–4106.
Rousseau, D. L., Ching, Y.-C., Brunori, M., & Giacometti, G. M. (1989) *J. Biol. Chem. 264*, 7878–7881.
Sage, J. T., Morikis, D., & Champion, P. M. (1989) *J. Chem. Phys. 90*, 3015–3032.
Sage, J. T., Li, P., & Champion, P. M. (1991) *Biochemistry* (following paper in this issue).
Sassaroli, M., & Rousseau, D. L. (1987) *Biochemistry 26*, 3092–3098.
Schomacker, K. T., Delaney, J. K., & Champion, P. M. (1986) *J. Chem. Phys. 85*, 4240–4247.
Shelnutt, J. A., Alston, K., Ho, J.-Y., Yu, N.-T., Yamamoto, T., & Rifkind, J. M. (1986) *Biochemistry 25*, 620–627.
Shen, L. L., & Hermans, J., Jr. (1972) *Biochemistry 11*, 1836–1849.
Shimada, H., & Caughey, W. S. (1982) *J. Biol. Chem. 257*, 11893–11900.
Sibbett, S. S., Loehr, T. M., & Hurst, J. K. (1986) *Inorg. Chem. 25*, 307–313.
Spiro, T. G., & Burke, J. M. (1976) *J. Am. Chem. Soc. 98*, 5482–5489.
Šrajer, V., Schomacker, K. T., & Champion, P. M. (1986) *Phys. Rev. Lett. 57*, 1267.
Šrajer, V., Reinisch, L., & Champion, P. M. (1988) *J. Am. Chem. Soc. 110*, 6656–6670.
Tanford, C. (1970) *Adv. Protein Chem. 24*, 1.
Teraoka, J., & Kitagawa, T. (1980) *J. Phys. Chem. 84*, 1928.
Teraoka, J., & Kitagawa, T. (1981) *J. Biol. Chem. 256*, 3969.
Traylor, T. G., Deardurff, L. A., Coletta, M., Ascenzi, P., Antonini, E., & Brunori, M. (1983) *J. Biol. Chem. 258*, 12147–12148.
Traylor, T. G., Koga, N., & Deardurff, L. A. (1985) *J. Am. Chem. Soc. 105*, 6504–6510.
Wang, C.-M., & Brinigar, W. S. (1979) *Biochemistry 18*, 4960–4977.
Warshel, A., & Weiss, R. M. (1981) *J. Am. Chem. Soc. 103*, 446–451.
Yu, N.-T., & Kerr, E. A. (1988) in *Applications of Raman Spectroscopy to Biological Systems* (Spiro, T. G., Ed.) pp 39–95, Wiley, New York.

Spectroscopic Studies of Myoglobin at Low pH: Heme Ligation Kinetics†

J. Timothy Sage, Pusheng Li, and Paul M. Champion*
Department of Physics, Northeastern University, Boston, Massachusetts 02115
Received May 14, 1990; Revised Manuscript Received October 11, 1990

ABSTRACT: On the basis of the characterization of heme structure and ligation in equilibrium, we explore both proximal and distal ligation kinetics of myoglobin below pH 4. Upon photolysis of MbCO, a significant five-coordinate heme population is observed, with an intact iron–histidine bond that persists on the time scale of CO rebinding. Incomplete CO photolysis is attributed to a rapidly exchanging minority population of four-coordinate hemes, which leads to fast ($>10^{10}$ s^{-1}) geminate recombination. The possible relevance of such a mechanism at pH 7 is also noted. Using a novel experimental protocol, we observe the resonance Raman spectrum of partially photolyzed MbCO as a function of continuous wave illumination time (τ). Under extended illumination ($\tau \sim 35$ ms at pH 3.4), there is a loss of intensity in the ν_4 region of the Raman spectrum and the iron–histidine mode is bleached from the spectrum of the five-coordinate photoproduct. In the Fe–CO stretching region of the CO-bound fraction, the intensity of the 526-cm^{-1} mode increases with τ at the expense of the 491-cm^{-1} mode. These changes are interpreted as being due to replacement of the proximal histidine ligand under continuous illumination. Complete relaxation to the pure four-coordinate deoxy heme structure observed in equilibrium is not observed even as $\tau \rightarrow \infty$, presumably since CO rebinding leads to acidification of the iron and its complexation with histidine. We propose a kinetic model to account for our results and discuss the implications for previous low-pH kinetics measurements.

Myoglobin has been widely utilized as a model system for studying the relationship between protein structure, dynamics, and function. Of particular interest is the means by which the protein modulates the rate of binding of small ligands such as CO to the heme. Motion of the iron into the heme plane is believed to make a significant contribution to the activation barrier that must be overcome upon ligand binding. The magnitude of this proximal contribution has been successfully described by a simple harmonic approximation to the iron out-of-plane motion (Šrajer et al., 1988). Distal contributions to ligand binding rates are also likely to be important, and interactions of the bound ligand with the distal histidine are believed to play a key role (Moffat et al., 1979; Doster et al., 1982; Nagai et al., 1987; Olson et al., 1988; Braunstein et al., 1988; Morikis et al., 1989).

Previous work has shown that ligand binding kinetics in myoglobin can be modulated by varying pH, and increased

†This work was supported by grants from NSF (87-16382) and NIH (AM-35090).

0006-2960/91/0430-1237$02.50/0